

Article

# Assessment of Soil Erosion in the Qinba Mountains of the Southern Shaanxi Province in China Using the RUSLE Model

Zhijie Wang <sup>1,2,\*</sup>  and Yuan Su <sup>3</sup>

<sup>1</sup> State Key Laboratory of Soil Erosion and Dryland Farming on the Loess Plateau, Institute of Water and Soil Conservation, Chinese Academy of Sciences and Ministry of Water Resources, Yangling 712100, China

<sup>2</sup> College of Life Sciences, Guizhou University, Guiyang 550025, China

<sup>3</sup> College of Forestry, Guizhou University, Guiyang 550025, China; ysu@gzu.edu.cn

\* Correspondence: zjwang3@gzu.edu.cn; Tel.: +86-0851-8842-0767

Received: 18 December 2019; Accepted: 25 February 2020; Published: 26 February 2020



**Abstract:** The Southern Shaanxi Province, an important ecological security barrier area in central China, is the primary water source of the south-to-north water transfer project in China. However, severe soil erosion seriously affects the safety of regional ecological security and water quality of the water diversion project. To reveal the characteristics and variation of soil erosion in the southern Shaanxi Province after the implementation of a series of eco-environmental construction measures, in this study, the spatio-temporal characteristics of soil erosion from 2000 to 2014 were evaluated based on the Revised Universal Soil Loss Equation (RUSLE) model and Geographic Information Systems (GIS). The average soil erosion of southern Shaanxi Province in China was characterized as slight (less than  $500 \text{ t}\cdot\text{km}^{-2}\cdot\text{a}^{-1}$ ) and mild erosion ( $500\text{--}2500 \text{ t}\cdot\text{km}^{-2}\cdot\text{a}^{-1}$ ) with an average soil erosion modulus of  $1443.49 \text{ t}\cdot\text{km}^{-2}\cdot\text{a}^{-1}$ ,  $1710.49 \text{ t}\cdot\text{km}^{-2}\cdot\text{a}^{-1}$ ,  $1771.99 \text{ t}\cdot\text{km}^{-2}\cdot\text{a}^{-1}$  and  $1647.74 \text{ t}\cdot\text{km}^{-2}\cdot\text{a}^{-1}$  in 2000, 2005, 2010 and 2014, respectively. The results revealed an increase in soil erosion until 2000 and a mitigation during the period of 2000 to 2014. After 2010, the soil erosion was controlled effectively. The spatial distribution of soil erosion displayed obvious spatial heterogeneity, and the high soil erosion (greater than  $2500 \text{ t}\cdot\text{km}^{-2}\cdot\text{a}^{-1}$ ) was primarily distributed in the north-central and south counties of the study area. The soil erosion remained high and aggravated in six counties (i.e., Zhen'an, Zhashui, Ningshan, Ningqiang, Lueyang and Shanyang), and high erosion (greater than  $5000 \text{ t}\cdot\text{km}^{-2}\cdot\text{a}^{-1}$ ) was found in the regions with slope gradients greater than 35 degrees and the middle mountainous (800–2000 m) regions. Therefore, the eco-environmental construction measures could effectively control soil erosion. However, unreasonable human activities remain the primary cause of soil erosion in the southern Shaanxi Province. In the future, more comprehensive and thorough ecological construction measures will be necessary to ensure regional ecological security and the eco-environmental quality of water sources.

**Keywords:** soil erosion; RUSLE model; south-to-north water transfer project; southern Shaanxi Province; Grain for Green program

## 1. Introduction

Soil erosion and its induced land degradation, as one of the most serious global environmental problems affecting human sustainable development, has attracted the extensive attention of policy makers and scholars [1,2]. China is one of the highest soil erosion regions in the world, with a soil erosion area reaching 29.49 million  $\text{km}^2$ , accounting for 30.7% of the total land area [3]. Many scholars have carried out researches on the monitoring and evaluation of soil erosion in China's Loess Plateau region [4–7], black soil region [8,9], purple soil region [10], the karst region [11,12], and the Qinghai-Tibet

Plateau region [13,14], among others. Meanwhile, the Chinese government has also implemented many comprehensive measures and projects to control soil erosion and to restore ecosystems. However, as the most important ecological security barrier area and the water source area of the Middle Route south-to-north water transfer project (MRSNWTP), the assessment of soil erosion in southern Shaanxi is very weak.

In fact, although southern Shaanxi has a good ecological background, abundant biodiversity and natural resources [15], for a long time, the economic development of the southern Shaanxi Province was backward, the ecological infrastructure was weak, and the problem of ecological environment deterioration was increasingly prominent [16]. At present, due to long-term reclamation and natural vegetation degradation, the ecological benefits of the mountainous areas are deteriorated, the function of regional ecological security is significantly reduced, and natural disasters caused by unreasonable human activities have become frequent [15,17,18]. According to the third soil erosion remote sensing survey of the Shaanxi Province, the soil and water loss area of the Hanjiang basin in the Shaanxi Province is approximately 34,000 km<sup>2</sup>, accounting for 54.1% of the basin area. The sediment discharge accounts for 12% of the Yangtze River watershed, with an average annual soil erosion amount of  $1.2 \times 10^8$  t, whereas the area of the Hanjiang basin only accounts for 4% of the total area of the Yangtze River watershed [19].

In order to protect the eco-environment of the water source area of the MRSNWTP and reduce soil and water loss, a larger number of comprehensive soil and water conservation measures have been carried out in the southern Shaanxi Province since 1981. Especially with the launch of the Grain for Green Program (GFG) in 1999, a series of soil and water loss control measures and projects, including afforestation, the abandonment of farmland on a slope above 25 degrees, and reforestation on barren mountains, and hillsides closed off for forest conservation and so on, have been implemented successively. Until 2018, the area of GFG has reached  $8.47 \times 10^3$  km<sup>2</sup>, and the forest coverage of the three cities (i.e., Ankang City, Shangluo City, and Hanzhong City) in the study area has increased from 39.2%, 52.4%, and 47.6% in 1999 to 65%, 66.50%, and 59.11%, respectively. However, after the implementation of many eco-environmental protection and construction measures, there is no in-depth quantitative study on soil erosion in the southern Shaanxi Province. Whether soil erosion has been controlled effectively in the southern Shaanxi Province, characterization of the spatiotemporal changes in soil erosion, and the key points of eco-environmental management and protection in the future are urgent scientific problems that must be solved. At present, scientific research on soil erosion in the southern Shaanxi Province is only focused on the plot scale [15], and some at a regional scale [19,20]. The systematic evaluations on soil erosion at a large scale are very few, and additional research is required.

Several empirical models, e.g., RUSLE (Revised Universal Soil Loss Equation) [21,22], or physical models, e.g., WEPP (Water Erosion Prediction Project) [23] and PESERA (Pan-European Soil Erosion Risk Assessment) [24], have been developed around the world [25]. RUSLE is one of the most widely used erosions models at the present stage [26], It is an empirical soil erosion model designed according to the Universal Soil Erosion Equation (USLE) [22]. The purpose of its development was to estimate the long-term average soil erosion [27]. The RUSLE model classified the influences on the soil erosion process into five groups, i.e., climate, soil, topography, vegetation, land use, and land management practices, which correspond to the rainfall erosivity factor (R), soil erodibility factor (K), slope length and Steepness factor (LS), cover management factor (C) and conservation practice factor (P), respectively [28]. Due to its simple and robust model form [27,29], RUSLE has been used in the prediction of soil loss at different spatial scales in different regions of the world [27,30–33]. In addition, the RUSLE model has strong compatibility with Geographic Information Systems (GIS), and it is easy to carry out spatial analysis with GIS [34,35]. RUSLE supported by GIS environment is considered as a reliable model for estimating annual soil loss based on pixel information, which not only has the advantages of being less time consuming and less expensive, but also provides a clear perspective for understanding the interaction between erosion and its contributing factors, presents the spatial heterogeneity of soil erosion, and identifies the spatial distribution and difference of erosion

areas [36–38]. Therefore, the RUSLE model has been the most widely and frequently used and globally accepted empirical model for soil erosion estimation worldwide.

Therefore, in this paper, with the southern Shaanxi Province in China as a case study, the RUSLE model combined with GIS technology was applied to assess the spatiotemporal distribution and to change characteristics of soil erosion from 2000 to 2014. The goal of the present study was to reveal the soil erosion change features during the study periods and provide information for decision-makers to implement appropriate land and/or environmental management strategies and land use planning within the Qinba Mountains of the southern Shaanxi Province in China.

## 2. Materials and Methods

### 2.1. Study Area

The study area ( $31^{\circ}42'–34^{\circ}45'$ ,  $105^{\circ}46'–111^{\circ}15'$ ) is the southern Shaanxi Province, China, that belongs to the Qinba Mountains region with the Qinling Mountains in the north and the Bashan Mountains in the south (Figure 1), and is also the primary water source of the MRSNWTP. The study area includes Hanzhong City, Ankang City and Shangluo City from west to east, respectively. The total area is approximately  $7.026 \times 10^4 \text{ km}^2$ , accounting for about 35% of the total area of the Shaanxi Province. The climate type in the region is the north subtropical monsoon climate area in the western part, and is the excessive area of the north subtropical and warm temperate zone. The average annual temperature is  $12–15^{\circ}\text{C}$  and the annual precipitation is  $700–1300 \text{ mm}$ . The main land-use areas are about  $6.19 \times 10^4 \text{ km}^2$  for woodland,  $6.69 \times 10^3 \text{ km}^2$  for agricultural land,  $1.26 \times 10^3 \text{ km}^2$  for construction land, and  $183 \text{ km}^2$  for water body, respectively, the natural forest area accounting for 45.1% of the total area. Crops (i.e., maize, wheat and rice), economic forests, sparse woods, and mixed needle and deciduous broadleaved types characterize the primary land uses [16].

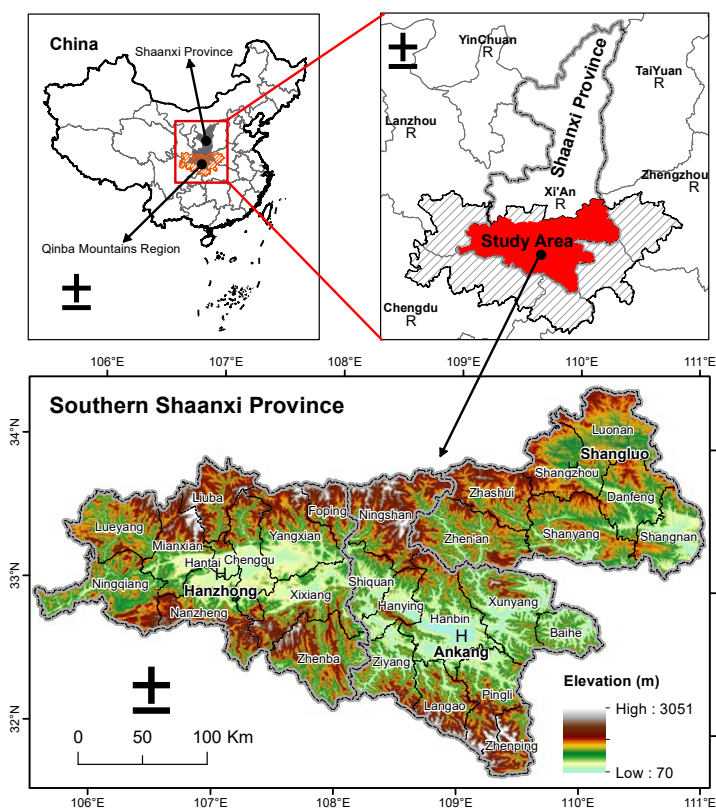


Figure 1. Location of study area.

## 2.2. Data Sources and Processing

### 2.2.1. Model Structure

In this study, the RUSLE model and GIS were applied to estimate the characteristics of soil erosion in the southern Shaanxi Province from 2000 to 2014. The formula of the RUSLE model is as follows:

$$A = R \times K \times LS \times C \times P, \tag{1}$$

where A is the average soil loss in  $t\ hm^{-1}\ a^{-1}$ , R is the rainfall erosivity factor in  $MJ\ mm\ a^{-1}\ h^{-1}\ a^{-1}$ , K is the soil erodibility factor in  $t\ hm\ h\ hm^{-1}\ MJ^{-1}\ mm^{-1}$ , LS is the topographic factor, C is the cover management factor, and P is the conservation practice factor. The L, S, C, and P factors are dimensionless.

### 2.2.2. Data Sources

According to the five factors of the RUSLE model, the main related data used in this study include the following: (1) Landsat TM remote sensing images in 2000, 2005, 2010 and 2014 were collected from the Data Sharing Infrastructure of Earth System Science (<http://www.geodata.cn>), with a spatial resolution of 30 m. The cloud content of each image was less than 5%, and the image quality was good. (2) DEM data, using SRTM (Shuttle Radar Topography Mission) data set with a spatial resolution of 30 m, was provided by the International Scientific and Technical Data Mirror Site, Chinese Academy of Sciences (<http://www.gscloud.cn/>). (3) Soil data sets, including soil type distribution map, soil organic carbon, and multi-layer soil particle size distribution data set in southern Shaanxi, were derived from the second soil investigation in China (<http://vdb3.soil.csdb.cn/>). (4) Daily rainfall data of 28 meteorological stations in the southern Shaanxi Province in 2000, 2005, 2010, and 2014 were obtained from the National Meteorological Information Center of China (<http://cdc.cma.gov.cn/>).

### 2.2.3. Data Processing

Referring to the methods of evaluating soil erosion by the RUSLE model of previous researches [4,6], all five factors of the RUSLE model in this study were calculated in the environment of GIS software with the calculation methods or equations of five factors detailed in the flowchart of data processing (Figure 2).

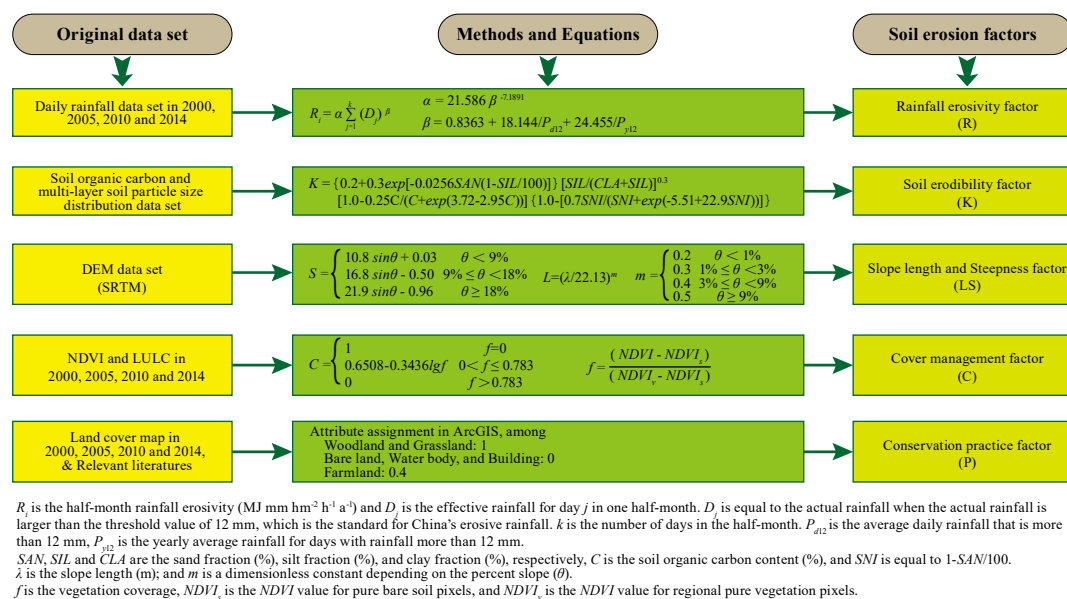


Figure 2. Flowchart of data processing for the Revised Universal Soil Loss Equation (RUSLE) model.

The rainfall erosivity factor (R) was calculated by using the method based on aggradations of half-month rainfall erosivity using daily rainfall data developed by [39] with the Inverse Distance Weighted (IDW) interpolation tool in the ArcGIS 10.2 software (Figure 3).

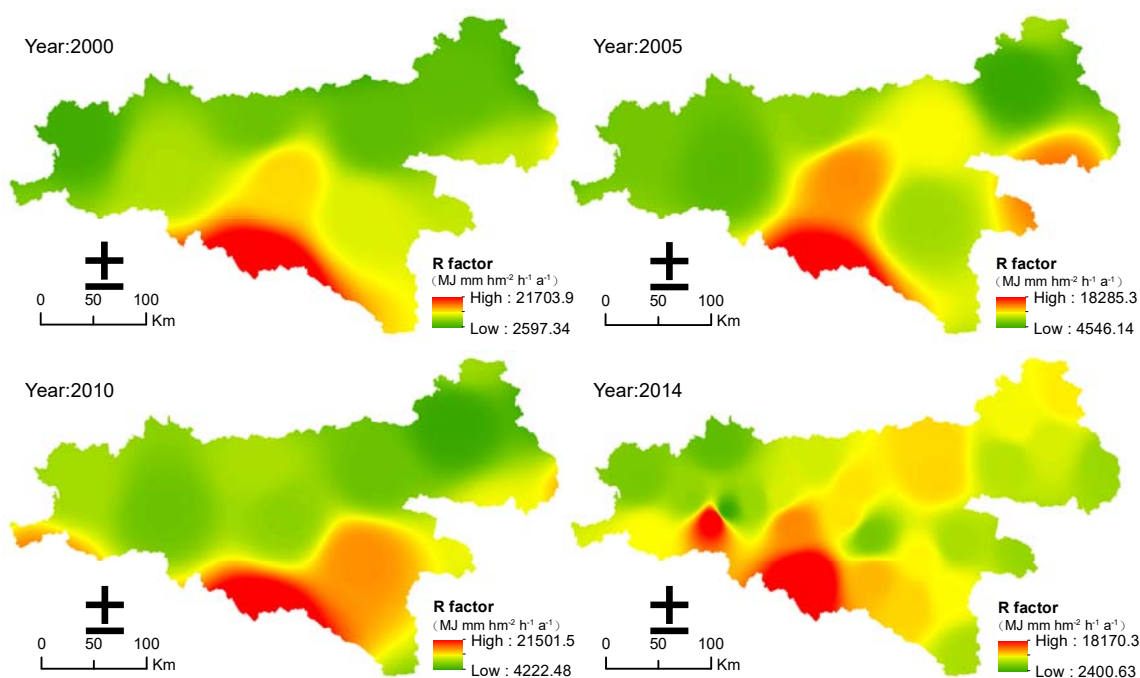


Figure 3. Rainfall erosivity map in 2000, 2005, 2010, and 2014.

The soil erodibility factor (K) of different soil types was calculated by Erosion-Productivity Impact Calculator (EPIC) equation proposed by [40] using the soil data sets of the study area. Then, the soil erodibility factor distribution map was obtained by using the distribution map of soil types in the study area and relating the K factor value to the attribution of the different soil types in the ArcGIS 10.2 software (Figure 4).

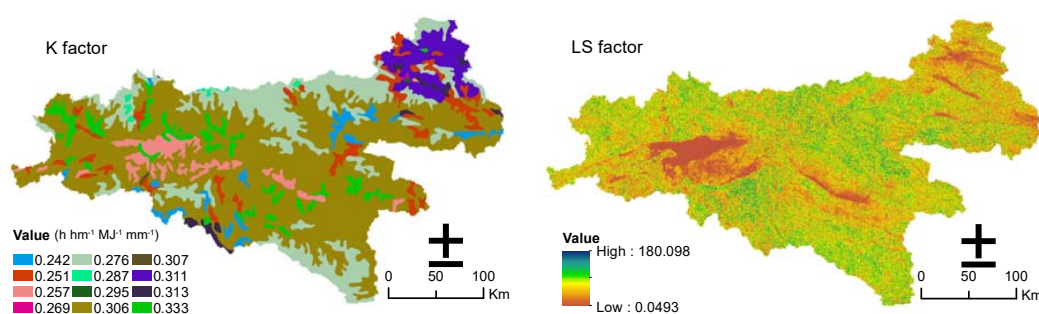
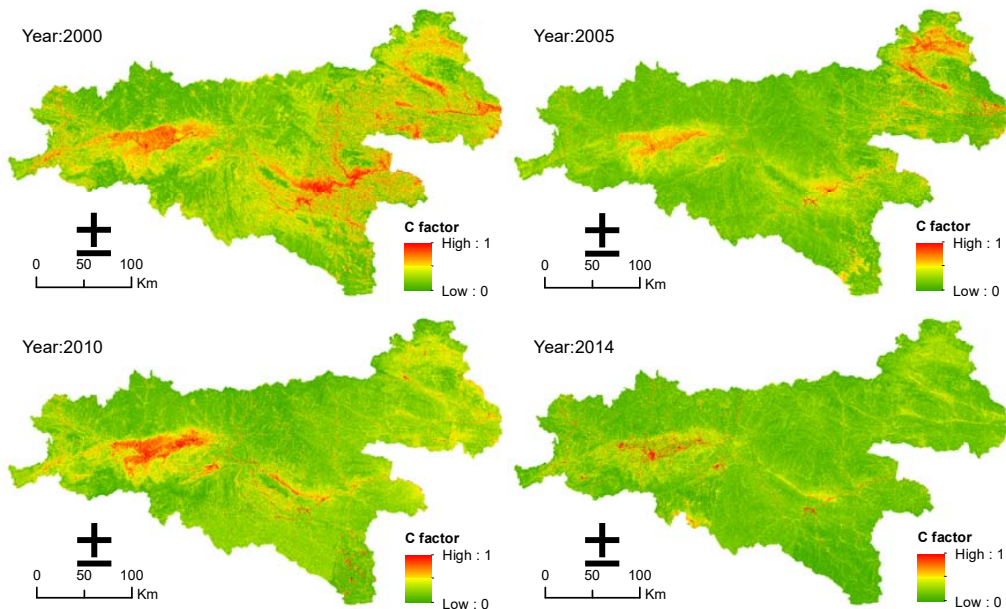


Figure 4. Soil erodibility factor (K factor) and slope length and steepness factor (LS factor) map of the southern Shaanxi Province.

In view of the limitation that the topographic factor (LS) algorithm in the RUSLE model was limited to slopes less than or equal to 18% [41], Ref [42] revised the LS calculation formula of slope between 9% and 55%. Therefore, the LS spatial distribution map of the study area (Figure 4) was obtained by using the modified algorithm developed by [42].

Due to the close relationship between the cover management factor (C) and vegetation coverage [43], the authors of [44] established a formula for estimating the cover management factor by using the Normalized Difference Vegetation Index (NDVI) and vegetation coverage. In this study, NDVI and

vegetation coverage of four periods in the study area were extracted by using Landsat TM remote sensing images in the ENVI 5.3 software platform, the formula proposed by [44] was used to obtain the spatial distribution maps of the coverage management factor in the study area (Figure 5).



**Figure 5.** Cover management factor (C factor) map of the southern Shaanxi Province in 2000, 2005, 2010, and 2014.

The conservation practice factor (P) was the most difficult determination factor in RUSLE [21]. Referring to relevant literatures, the study used land use and cover maps of different periods in the study area to roughly determine the conservation practice factor by an attribute assignment method in the ArcGIS 10.2 software, and obtained the spatial distribution maps of the conservation practice factor of the study area (Figure 6).

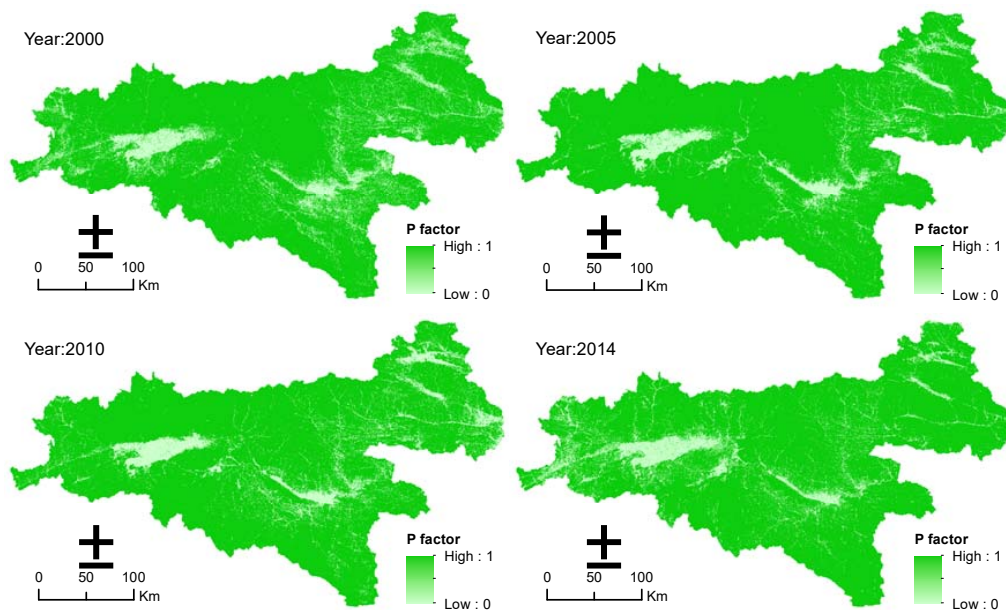


**Figure 6.** Conservation practice factor (P factor) map of the southern Shaanxi Province in 2000, 2005, 2010, and 2014.

Among them, the land use and cover maps were obtained by the maximum likelihood supervised classification method in the ENVI 5.3 software platform. The land use types were classified into woodland, grassland, bare land, water body, buildings, and farmland. In addition, prior to the implementation of supervised classification of land use types, all the remote sensing images in this study were pre-processed by geometric correction, image mosaic, and image clipping, etc. The geometric correction was carried out with reference to the 1:10,000 relief map of the study area based on the quadratic polynomial correction method, with the RMS error less than one pixel. Furthermore, the coordinate system of the spatial distribution maps of all five factors was unified into WGS\_1984\_UTM\_Zone\_49N by the re-projection method, with a spatial resolution of 30 m.

After obtaining the spatial distribution maps of five factors of the study area, the soil erosion intensity in different periods of the southern Shaanxi Province was calculated using the raster calculation tools based on the ArcGIS 10.2 software platform. Then, according to the classification standard of soil erosion intensity in China (SL190-2007), the soil erosion intensity was divided into six levels, namely, slight erosion (less than  $500 \text{ t}\cdot\text{km}^{-2}\cdot\text{a}^{-1}$ ), mild erosion ( $500\text{--}2500 \text{ t}\cdot\text{km}^{-2}\cdot\text{a}^{-1}$ ), moderate erosion ( $2500\text{--}5000 \text{ t}\cdot\text{km}^{-2}\cdot\text{a}^{-1}$ ), strong erosion ( $5000\text{--}8000 \text{ t}\cdot\text{km}^{-2}\cdot\text{a}^{-1}$ ), very strong erosion ( $8000\text{--}15,000 \text{ t}\cdot\text{km}^{-2}\cdot\text{a}^{-1}$ ), and severe erosion (greater than  $15,000 \text{ t}\cdot\text{km}^{-2}\cdot\text{a}^{-1}$ ), to analyze the spatial and temporal characteristics of soil erosion.

To reveal the impact of rainfall and vegetation on soil erosion change, the soil erosion modulus of different periods was calculated in three scenarios: natural state, R factor fixation and C factor fixation. By comparing the average soil erosion modulus under R factor fixation and C factor fixation scenarios with the actual average soil erosion modulus under the natural state, the change amount, the change rate and the contribution rate of rainfall and vegetation on soil erosion was analyzed. The calculation formulas are as follows:

$$Asp_i = R_i \times K \times LS \times C_i \times P_i \quad (2)$$

$$AR_j = R_j \times K \times LS \times C_i \times P_i \quad (3)$$

$$AC_j = R_i \times K \times LS \times C_j \times P_i \quad (4)$$

where  $Asp_i$  is the soil erosion modulus under the natural state in the initial year in the periods of 2000–2005, 2005–2010, 2010–2014 and 2000–2014, i.e., the actual soil erosion modulus in 2000, 2005 and 2010.  $AR_j$  is the soil erosion modulus calculated by the R factor value using the end year of each period, while other factors maintain at the initial year of each periods.  $AC_j$  is the soil erosion modulus calculated by the C factor value using the end year of each period, while other factors maintain at the initial year of each periods.  $i$  is the initial year of each period,  $j$  is the end year of each period.

### 3. Results

#### 3.1. Characteristics of Different Soil Erosion Intensity

Figure 7 and Table 1 show the soil erosion modulus and distribution of the study area in 2000, 2005, 2010, and 2014. In the past 15 years, the soil erosion intensity in most of the study area was classified with slight and mild erosion, which accounted for more than 80% of the total area. The distribution of strong, very strong and severe erosion was less in the study area and accounted for approximately 3% of the total area. The average annual soil erosion modulus increased from 2000 to 2010 and then decreased from 2010 to 2014 with an average of  $1443.49 \text{ t}\cdot\text{km}^{-2}\cdot\text{a}^{-1}$ ,  $1710.49 \text{ t}\cdot\text{km}^{-2}\cdot\text{a}^{-1}$ ,  $1771.99 \text{ t}\cdot\text{km}^{-2}\cdot\text{a}^{-1}$  and  $1647.74 \text{ t}\cdot\text{km}^{-2}\cdot\text{a}^{-1}$  in 2000, 2005, 2010 and 2014, respectively.

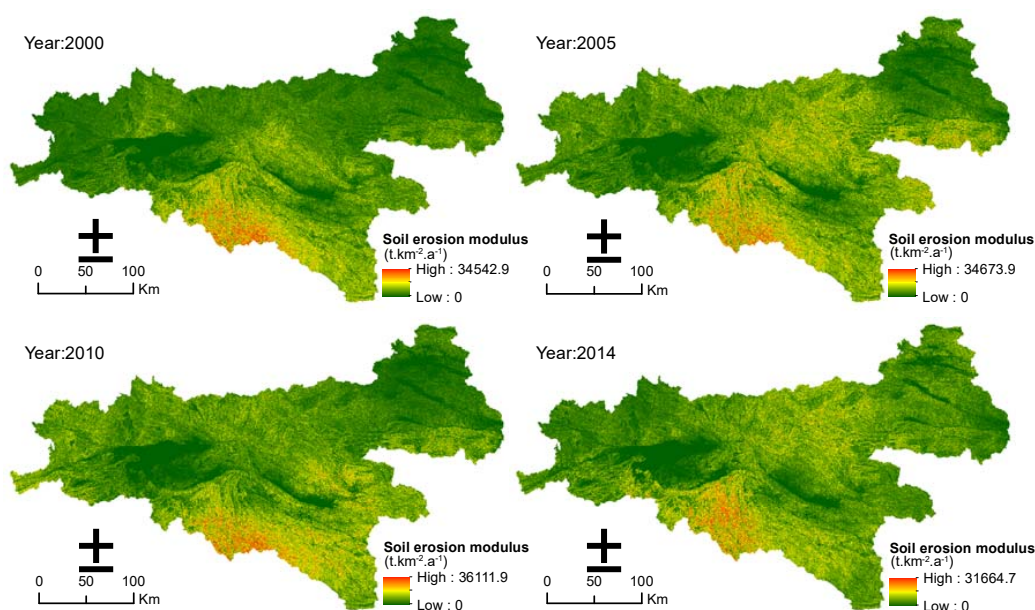


**Figure 7.** Soil erosion modulus of the southern Shaanxi Province in 2000, 2005, 2010, and 2014.

**Table 1.** The area and percent of different soil erosion intensity of in 2000, 2005, 2010, and 2014.

Erosion Intensity	2000		2005		2010		2014	
	Area (km <sup>2</sup> )	Percent (%)						
Slight	328.54	46.77	240.77	34.28	240.62	34.26	244.68	34.83
Mild	266.72	37.97	307.87	43.83	298.03	42.43	321.39	45.75
Moderate	89.30	12.71	136.49	19.43	140.58	20.01	120.92	17.21
Strong	14.87	2.12	15.77	2.25	20.35	2.90	13.56	1.93
Very strong	3.00	0.43	1.52	0.22	2.80	0.40	1.98	0.28
Severe	0.07	0.01	0.02	0.00	0.05	0.01	0.03	0.00

From 2000 to 2005, the areas of slight erosion, very strong erosion and severe erosion were reduced with amplitude reductions of 26.71%, 49.27% and 75.30%, respectively. The area of the other levels of soil erosion intensity increased, and the moderate erosion level had the largest amplification of 52.83%. From 2005 to 2010, the areas of slight and mild erosion decreased, with amplitude reductions of 0.06% and 3.20%, respectively. The areas of moderate erosion, strong erosion, very strong erosion, and severe erosion increased with amplifications of 3.00%, 29.03%, 83.83% and 204.04%, respectively. The areas of very strong and severe erosion in 2010 were higher than those in 2005. However, from 2010 to 2014, the areas of slight erosion and mild erosion increased slightly with amplifications of 1.69% and 7.84%, respectively. By contrast, the areas of moderate erosion, strong erosion, very strong erosion, and severe erosion clearly decreased, with amplitude reductions of 13.99%, 33.37%, 29.32%, and 39.18%, respectively. Overall, compared with 2000, except for areas of mild erosion and moderate erosion, the areas of slight erosion, strong erosion, very strong erosion and severe erosion decreased to different extents in 2014. Therefore, although the average soil erosion modulus increased in these recent 15 years, the area of very strong and severe erosion was clearly reduced, and the soil erosion in the study area was controlled effectively.

### 3.2. Change Detection of Different Soil Erosion Intensities

The change maps were obtained by overlaying the soil erosion intensity images of 2000, 2005, 2010, and 2014. The resultant change maps displayed “from-to” the soil erosion intensity changes (Figure 8). In the period of 2000 to 2005, the soil erosion intensity area of regions with no changes (NC), increases, and decreases was 45,214.52 km<sup>2</sup>, 18,753.33 km<sup>2</sup> and 6257.12 km<sup>2</sup>, respectively. The proration

of the increased region accounted for 26.70% of the total area and was approximately three-fold more than that of the reduced region. The region with an increase was primarily because of the transfer from slight erosion to mild erosion and mild erosion to moderate erosion with the proration of 59.26% and 32.66% of the total increased region area, respectively. Additionally, the erosion was distributed in seven counties with an area percentage greater than 55% of the total increased region area, i.e., Zhen'an, Lueyang, Ningshan, Zhashui, Shanyang, Ningqiang and Xunyang. The reduced region was primarily because of the transfer from mild erosion to slight erosion, moderate erosion to mild erosion, and strong erosion to moderate erosion with the proration of 47.15%, 35.19%, and 11.62%, respectively. It was also primarily distributed in seven counties with an area percentage greater than 60% of the total reduced region area, i.e., Zhenba, Ziyang, Hanbin, Nanzheng, Pingli, Langao, and Xixiang.

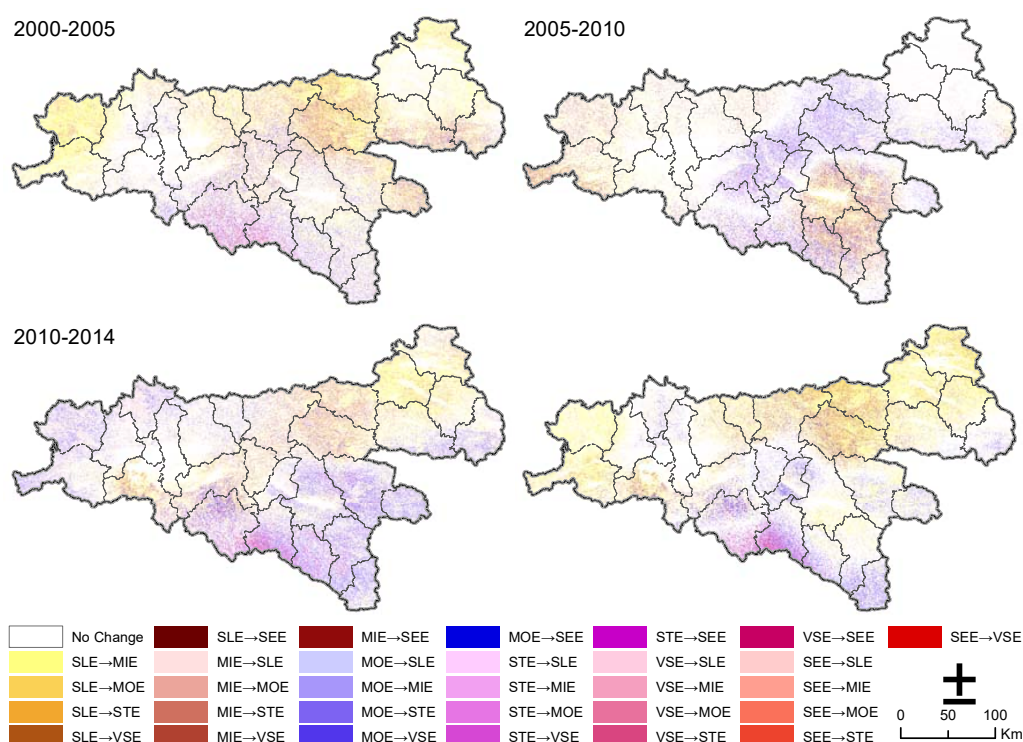


**Figure 8.** The spatial transfer changes of different soil erosion intensity levels in different periods. SLE: slight erosion, MIE: mild erosion, MOE: moderate erosion, STE: strong erosion, VSE: very strong erosion, SEE: severe erosion, No Change means the soil erosion intensity area of regions with no changes, right arrow means “from-to”.

Compared with 2000–2005, the worsening of soil erosion slowed in the 2005–2010 period. The area percentage of the no change, increased and reduced regions accounted for 76.5%, 12.94%, and 10.56%, respectively, of the total area. The increased region was primarily because of the transfer from mild erosion to moderate erosion, slight erosion to mild erosion, and moderate erosion to strong erosion with a proration of 51.37%, 33.20%, and 12.24% of the total increased region area, respectively. Additionally, it was primarily distributed (greater than 60%) in Pingli, Ningqiang, Hanbin, Xunyang and Lan’gao. The reduced region was primarily because of the transfer from moderate erosion to mild erosion, mild erosion to slight erosion, and strong erosion to moderate erosion with a proration of 50.00%, 41.03%, and 7.16%, respectively, of the total reduced region area. It was primarily distributed (greater than 65%) in Zhen’an, Zhashui, Shiquan, Ningshan, Xixiang and Shanyang.

In the period of 2010 to 2014, the soil erosion was controlled effectively; the area percentage of the reduced region was larger than that of the increased region with prorations of 21.45% and 16.14%, respectively. The increased region was primarily because of the transfer from slight erosion to mild erosion, mild erosion to moderate erosion, and moderate erosion to strong erosion with the

proration of 52.23%, 38.64%, and 6.02% of the total increased region area, respectively. It was primarily distributed (greater than 60%) in Zhen'an, Shangzhou, Zhashui, Ningshan, Xixiang, Nanzheng and Zhenba. The reduced region was primarily because of the transfer from moderate erosion to mild erosion, mild erosion to slight erosion, and strong erosion to moderate erosion with the proration of 45.71%, 41.08%, and 8.86% of the total reduced region, respectively. Additionally, it was primarily distributed (greater than 70%) in Xunyang, Lueyang, Hanbin, Pingli, Ningqiang, Ziyang, Langao, Liuba, Baihe, and Shangnan.

Overall, in these recent 15 years, the transfer of the soil erosion intensity in the study area primarily occurred among slight, mild, moderate, and strong levels of erosion. The obvious change regions for soil erosion intensity were primarily concentrated in 14 counties, i.e., Lueyang, Nanzheng, Shanyang, Zhenba, Ziyang, Hanbin, Langao, Ningqiang, Ningshan, Pingli, Xixiang, Xunyang, Zhashui and Zhen'an. Among these counties, soil erosion in Ziyang, Hanbin, Zhenba, Langao, Pingli and Xunyang was controlled effectively after many years of eco-environmental restoration and construction. However, the soil erosion in Zhen'an, Zhashui, Ningshan, Ningqiang, Lueyang and Shanyang underwent fluctuations and has currently not slowed down.

### 3.3. Distribution and Dynamic Changes of Soil Erosion Intensity on Slope Gradients

In the present study, the slope gradients were classified into six levels, i.e.,  $<5^\circ$ ,  $5^\circ\text{--}15^\circ$ ,  $15^\circ\text{--}25^\circ$ ,  $25^\circ\text{--}35^\circ$ ,  $35^\circ\text{--}45^\circ$ , and  $>45^\circ$ . Figure 9a displays the distribution and changes in soil erosion intensity on different slope gradients. The result showed that the highest soil erosion was distributed at high slope gradient levels. For example, the average area ratio greater than 75% of each soil erosion intensity level in different years was distributed in  $5^\circ\text{--}25^\circ$ ,  $15^\circ\text{--}35^\circ$ ,  $25^\circ\text{--}45^\circ$ ,  $>35^\circ$ , and  $>45^\circ$  slope levels. Furthermore, each soil erosion intensity level experienced irregular changes from 2000 to 2014. The area of slight and mild erosion at more than a  $25^\circ$  slope gradient level in 2014 decreased compared with that in 2000. However, the area of moderate, strong, very strong and severe erosion at more than a  $35^\circ$  slope gradient level in 2014 increased compared with that in 2000. In particular, the area ratio of strong erosion, very strong erosion and severe erosion at more than  $35^\circ$  slope levels increased from 53.06%, 80.67%, and 97.82% in 2000, to 70.35%, 94.94%, and 99.33% in 2014, respectively. This finding indicates that the soil erosion at the high slope levels (above  $35^\circ$ ) did not slow down, although eco-environmental restoration policies such as those of the Grain for Green program have been conducted in the study area since 1999 and state that slopes greater than  $25^\circ$  must return farmland to forest or grass to reduce soil erosion.

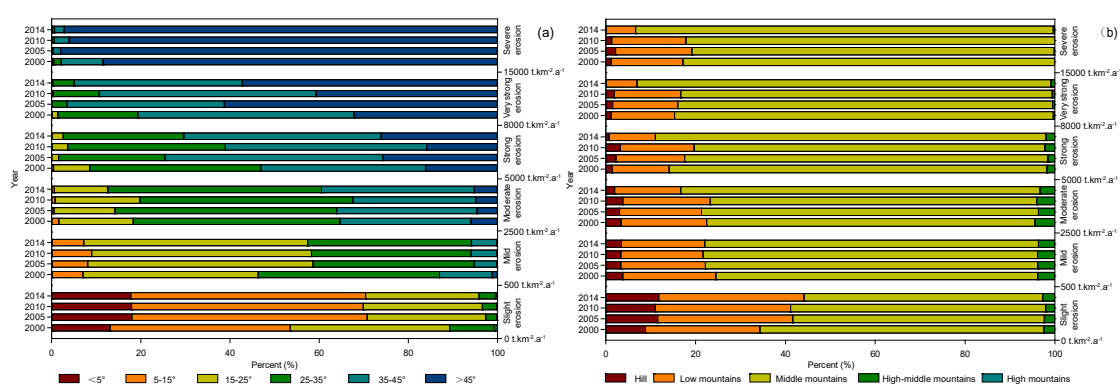


**Figure 9.** Distribution and changes of each soil erosion intensity levels in different slope gradients (a) and in different elevation gradients (b).

### 3.4. Distribution and Dynamic Changes of Soil Erosion Intensity at Different Elevations

The area percentage and changes in each soil erosion intensity level at different elevations are displayed in Figure 9b. Approximately 53–93% of the area of each erosion intensity level in the recent 15 years occurred in the middle mountainous (800–2000 m) region. Particularly for strong, very strong,

and severe erosion, more than 80% of the area ratio of these three levels of soil erosion intensity was distributed in the middle mountainous region. Moreover, 6–30% of each soil erosion intensity level was distributed in the hill (less than 500 m) and low mountainous (500–800 m) region. However, the distribution of each soil erosion level in the middle-high mountainous (2000–3000 m) region, high mountainous (3000–5000 m) region, and hill-gully region was less with an area percentage less than 5%. For the area percentage changes of each soil erosion intensity level at different elevations, all soil erosion intensity levels experienced irregular changes from 2000 to 2014. Additionally, the changes were more obvious in the period from 2010 to 2014 than those in the periods from 2000 to 2005 and 2005 to 2010. Except for the slight erosion level, the area percentage of mild, moderate, strong, very strong and severe erosion in 2014 declined in the hill-gully region and low mountainous region, increased in the middle mountainous region and middle-high mountainous region, and was inconspicuous in the high mountainous region, compared with that at 2000. The amplitude reduction or amplification of the five soil erosion intensity levels mild, moderate, strong, very strong and severe erosion was  $-8.35\%$ ,  $-41.88\%$ ,  $-47.65\%$ ,  $-87.38\%$ , and  $-88.15\%$  in the hill-gully region, respectively,  $-10.31\%$ ,  $-22.66\%$ ,  $-19.11\%$ ,  $-52.03\%$ , and  $-59.53\%$  in the low mountainous region, respectively,  $3.67\%$ ,  $9.42\%$ ,  $3.51\%$ ,  $9.36\%$ , and  $12.40\%$  in the middle mountainous region, respectively, and  $-4.76\%$ ,  $-25.82\%$ ,  $9.56\%$ ,  $150.12\%$ , and  $31,913.97\%$  in the middle-high mountainous region, respectively.

### 3.5. Effects of Precipitation and Vegetation for Soil Erosion Changes

Table 2 shows the influence of the rainfall erosivity factor (R) and vegetation cover factor (C) on average soil erosion modulus in different periods. It displayed that from 2000 to 2005, because of the change of rainfall erosivity factors, the average soil erosion modulus increased by 307, while the change of vegetation coverage factors caused by ecological restoration measures reduced the average soil erosion modulus by 57.60. From 2005 to 2010, compared with 2005, both the change of R factor and C factor resulted in an increasement of the average soil erosion modulus by 4.35% and 0.35%, respectively. However, from 2010 to 2014, Both the R factor and C factor reduced the average soil erosion modulus by  $106.02 \text{ t}\cdot\text{km}^{-2}\cdot\text{a}^{-1}$  and  $13.65 \text{ t}\cdot\text{km}^{-2}\cdot\text{a}^{-1}$ , respectively. In general, in the past 15 years, compared with the average soil erosion modulus at 2000, the change of R factors aggravated soil erosion, resulting in an increase of  $268.24 \text{ t}\cdot\text{km}^{-2}\cdot\text{a}^{-1}$  in the average soil erosion modulus, while C factors effectively slowed down the deterioration trend of soil erosion and reduced the average soil erosion modulus by about 62.66%. In addition, according to the contribution rate of R factor and C factor to the changes of soil erosion in the different periods, the contribution of R factor to the change of soil erosion was about 81.06–92.16%, while that of C factor was about 7.84–18.94%.

**Table 2.** The influence of R factor and C factor to soil erosion changes in different periods.

Periods	Asp ( $\text{t}\cdot\text{km}^{-2}\cdot\text{a}^{-1}$ )	AR ( $\text{t}\cdot\text{km}^{-2}\cdot\text{a}^{-1}$ )	AC ( $\text{t}\cdot\text{km}^{-2}\cdot\text{a}^{-1}$ )	AR-Asp ( $\text{t}\cdot\text{km}^{-2}\cdot\text{a}^{-1}$ )	AC-Asp ( $\text{t}\cdot\text{km}^{-2}\cdot\text{a}^{-1}$ )	CRR (%)	CRC (%)	CR (%)	CC (%)
2000–2005	1443.49	1751.02	1385.90	307.53	-57.60	21.30	-3.99	84.22	15.78
2005–2010	1710.49	1781.07	1716.50	70.58	6.00	4.13	0.35	92.16	7.84
2010–2014	1771.98	1665.97	1758.34	-106.02	-13.65	-5.98	-0.77	88.60	11.40
2000–2014	1443.49	1711.73	1380.83	268.24	-62.66	18.58	-4.34	81.06	19.84

Asp: average soil erosion modulus of the initial year in different periods, AR: average soil erosion modulus calculated by the R factor value using the end year of each period, while other factors are constant at the initial year of each period, AC: average soil erosion modulus calculated by the C factor value using the end year of each period, while other factors constant at the initial year of each period, CRR: change rate of the average soil erosion modulus caused by R factor, CRC: change rate of the average soil erosion modulus caused by C factor, CR: contribution rate of R factor for soil erosion change, CC: contribution rate of C factor for soil erosion change.

## 4. Discussion

In the most recent 15 years of this study, the average soil erosion of the southern Shaanxi Province in China was characterized as slight and mild erosion, which accounted for more than 80% of the total area. Additionally, the spatial distribution of soil erosion showed obvious spatial heterogeneity, and the areas with high soil erosion were primarily distributed in the north-central and south counties of the study

area, i.e., Ningshan, Zhashui, Zhen'an, Shanyang, Zhenba, Ziyang, and Langao (Figure 8). This might be related to the spatial heterogeneity of rainfall erosivity, topographic factors, and unreasonable human activities in the study area [6,45]. Combining the distribution map of rainfall erosivity, which accorded well with the spatial distribution of average annual rainfall [46] and soil erosion in the study area, the areas of high soil erosion were basically consistent with those of relatively high rainfall erosivity (Figure 3, Figure 7). It has been considered that soil erosion is more sensitive to rainfall, and rainfall erosivity is one of the most important climatic factors and parameters to determine soil erosion [32]. While other factors are constant and only the R factor changes, soil erosion is directly proportional to rainfall erosivity [36]. In the present study, the influence of rainfall erosivity on soil erosion in different periods indicated that the contribution of rainfall erosivity to soil erosion was more than 80% (Table 2). Moreover, the topographic factor might be another reason that caused this feature. Previous studies in other regions of China have found that slope is one of the important factors that affect soil erosion, where the steeper the slope, the higher the soil erosion [47]. In this study, the areas of relatively high soil erosion were primarily distributed in locations with high LS values (Figure 4, Figure 7), and the distribution of different soil erosion intensity levels on the slope gradients also displayed these characters (Figure 9a). Furthermore, unreasonable human activities might be another important reason that caused the spatial heterogeneity of soil erosion, although large-scale eco-environmental measures have been implemented in the southern Shaanxi Province. Because of the industrial development and population increase, coupled with a relatively low economic level, the phenomena of human activities and destruction of the ecological environment (i.e., deforestation, damaging forests to reclaim land) are persistent, particularly in the mid-mountain regions with relatively large slope gradients [19]. As a result, a state of relatively high soil erosion persists in north-central, southern and western regions of the study area. On the other hand, the RUSLE equation might give some extremely high values, and lead into an overestimation of erosion [26]. For example, previous studies in the southern Italy shown that the RUSLE model tend to amplify and emphasize the measured data, and the mean values of sediment yield from the *Tu index* (mean annual suspended sediment yield) and USPED (Unit Stream Power Erosion Deposition) method for the sub basins are very close and comparable, whereas the sediment yield coming from RUSLE method is much higher [48–50]. Thus, while the use of the RUSLE model evaluated the actual soil erosion of the study area, it should be supported by experimental measurements to reach a more objective analysis in the future.

From 2000 to 2014, the soil erosion changes in the study area showed deterioration first and then a slowing down, and after 2010, soil erosion was controlled effectively. It was closely related with a series of numerous eco-environmental construction measures in the southern Shaanxi Province, particularly those associated with the GFG program launched in 1999. Previous studies in the southern Shaanxi Province show that after the execution of the GFG program, many sloping farmlands with high soil erosion were transferred to woodland or grassland, with the rapid recovery of the vegetation and quickly improved vegetation coverage. High vegetation coverage can effectively reduce soil erosion [51]. Vegetation can reduce the impact of precipitation energy, increase soil infiltration, and reduce runoff and sediment [43], thereby reducing the surface erodibility and soil erosion risk [7]. In other words, vegetation restoration can reduce soil erosion sensitivity by improving the effectiveness of land cover [7]. This might be an important reason for the obvious reduction in soil erosion in southern Shaanxi since 2010. Research on the effects of the GFG program on soil erosion in other regions of China also found that returning farmland to forests effectively reduces soil erosion [4]. This result is consistent with the results in this study. However, another notable phenomenon was that although many eco-environmental construction measures have been implemented in the study area since 1999, soil erosion was not slowed down until 2010. Two possible reasons might explain this result. On one hand, in areas with high soil erosion, it takes a long time for the natural succession of vegetation to establish a stable vegetation cover, so as to exert good soil and water conservation effects [52,53]. On the other hand, with the development of the social economy and the increase in population, the southern Shaanxi Province progressed through a critical period of rapid development in recent

years. Previous studies shown that the land use structure of the study region changed significantly in 2000–2005 with a trend of the area of forest land increasing rapidly due to the influence of the policy of the GFG program, and the area of the agricultural land transferring to woodland reached 3663.40 km<sup>2</sup>. However, after 2005, many infrastructure projects were conducted to expand the scale of cities and improve the living standards of residents. Moreover, the phenomenon of deforestation was spreading again, the area of the woodland transferred to agricultural land and construction land reached 2991.44 km<sup>2</sup> and 79.11 km<sup>2</sup> respectively, while the area of agricultural land transferred to woodland was only 1343.89 km<sup>2</sup> in 2005–2010. It caused a certain degree of vegetation degradation and aggravation of soil erosion in this region [19,54]. The average soil erosion modulus increased by 0.35% in the study area due to the change of C factors in 2005–2010, and indirectly indicated the negative effects of vegetation destruction or degradation on soil erosion also (Table 2). Therefore, before 2010, the southern Shaanxi Province experienced the processes of both eco-environmental construction and protection and eco-environmental destruction and unreasonable interference. This might be also an important possible reason that soil erosion in counties such as Zhen'an, Zhashui, Ningshan, Ningqiang, Lueyang and Shanyang was not effectively controlled (Figure 8).

The distribution of soil erosion on different slope gradients showed that with a high slope gradient, high soil erosion occurred. Additionally, the primary areas with high soil erosion were areas with a slope gradient greater than 25 degrees. It was similar to studies in other regions of China [2,4,55]. Moreover, the area of soil erosion intensity above 2500 t·km<sup>-1</sup>·a<sup>-1</sup> on slope gradients greater than 35 degrees increased in the last 15 years. It confirmed that the slope steepness has a greater effect on soil loss, and with steep slopes, the erosion increases [32]. Especially for the cultivated land on steep land in the study area. According to the statistical data of Ankang City in 2004, the area of cultivated land with the slope of 25–35 degrees and greater than 35 degrees was 1424.13 km<sup>2</sup> and 407.76 km<sup>2</sup>, respectively, while the soil thickness is only 30–50 cm. Thus, the soil erosion risk in these areas is very high in case of rainstorm or heavy rainstorm. However, it might also be related to the deficiencies and limitations of the RUSLE model. Because the data used to develop RUSLE only included slopes up to 10%, the LS factor algorithms in the RUSLE model were limited to slopes less than 18% [41]. Although according to the wide distribution of steep slopes in China, Liu et al. [42] fixed the formula using soil loss data from natural runoff plots with slopes ranging from 9% to 55%, the output value of RUSLE might still be overestimated for the steep slopes. The comparative study of the predictions of soil erosion rates between RUSLE and PESERA for a wildfire in Greece found that RUSLE predictions were most sensitive to the topographic factor, and provided extremely high soil erosion predictions, particularly for areas with slope values greater than 60% which were one order of magnitude higher than the output values of PESERA [26]. In addition, previous research has suggested that the high soil erosion in the southern Shaanxi Province is primarily distributed in low hill regions in which human activities are relatively intense [17]. However, the results in this study displayed that the high soil erosion was primarily distributed in middle mountainous regions, followed by low mountainous regions. This is because the soil erosion in low hill regions has been obviously controlled under the influence of eco-environmental protection measures [19]. Meanwhile, the cities and population of the study area are mainly distributed in low and hilly mountainous regions, and due to the social and economic development of these regions in recent years, a large number of agricultural land has been converted into construction land, which forced many unreasonable human intervention activities like deforestation and reclamation spreading to middle mountainous regions [54], causing soil erosion in the middle mountainous regions to be relatively high at the current stage.

## 5. Conclusions

The spatio-temporal changes of soil erosion in the southern Shaanxi Province from 2000 to 2014 was evaluated by using RUSLE integrated with GIS. Based on this study, we concluded that the soil erosion in the southern Shaanxi Province was primarily characterized as slight erosion and mild erosion with the average soil erosion modulus ranging from 1443.49 to 1771.99 t·km<sup>-2</sup>·a<sup>-1</sup> from 2000 to 2014, and

was relatively high in the counties in the north-central, south, and west of the study area. Moreover, the rainfall erosivity factor (R) was the dominant and controlling factor of soil erosion change in the study area with its contribution rate to soil erosion of more than 80%, while the vegetation coverage factor (C) played a positive role in slowing down soil erosion, with its contribution rate close to 20%.

Under the influence of the GFG program launched in 1999, the soil erosion in the southern Shaanxi Province has been controlled effectively overall since 2010. However, although the comprehensive soil and water conservation measures, such as returning farmland to forest and returning all farmland above 25 degrees to farmland, have been vigorously implemented, erosion remained high and aggravated in six counties due to the impact of rapid socio-economic development and irrational human activities (i.e., Zhen'an, Zhashui, Ningshan, Ningqiang, Lueyang and Shanyang). Moreover, the regions with a slope gradient greater than 35 degrees and middle mountainous regions showed high erosion at the current stage.

The eco-environmental construction and protection measures or programs in southern Shaanxi Province should focus on the abovementioned regions in the future, to achieve comprehensive control of soil erosion, guarantee improvement in the regional ecological environment, and realize the ecological security and sustainable development of the water source of MRSNWTP in China.

The RUSLE model and GIS technology were adopted in this study to assess the soil erosion and its spatiotemporal heterogeneity in the southern Shaanxi Province. The methods and results are valuable in explaining the relationship between soil erosion and environmental factors, and also have guiding significance for planning land use to reduce soil erosion in this region. However, due to the lack of quantitative research on sediment yield and erosion rate the southern Shaanxi Province, further studies are necessary to quantitatively reveal soil erosion and its influencing factors, and to validate the performance of the RUSLE model in the field.

**Author Contributions:** Conceptualization, Z.W. and Y.S.; methodology, Z.W. and Y.S.; software, Z.W.; validation, Z.W. and Y.S.; formal analysis, Z.W.; investigation, Z.W. and Y.S.; resources, Z.W. and Y.S.; data curation, Y.S.; writing—original draft preparation, Z.W.; writing—review and editing, Z.W. and Y.S.; visualization, Z.W.; supervision, Z.W.; project administration, Z.W.; funding acquisition, Z.W. All authors have read and agreed to the published version of the manuscript.

**Funding:** This research was funded by Open Fund of State Key Laboratory of Soil Erosion and Dryland Farming on the Loess Plateau, grant number A314021402-1704, National Nature Science Foundation of China (NSFC) project, grant number 41701319, Key Science and Technology Program of Guizhou Province, China, grant number [2017]2854, and Research project of introducing talents in Guizhou University, grant number (2016)36.

**Acknowledgments:** We thank Jing YAO for her efforts in data collecting and processing.

**Conflicts of Interest:** The authors declare no conflict of interest.

## References

1. Mukanov, Y.; Chen, Y.; Baisholanov, S.; Amanambu, A.C.; Issanova, G.; Abenova, A.; Fang, G.; Abayev, N. Estimation of annual average soil loss using the Revised Universal Soil Loss Equation (RUSLE) integrated in a Geographical Information System (GIS) of the Esil River basin (ERB), Kazakhstan. *Acta Geophys.* **2019**, *67*, 921–938. [[CrossRef](#)]
2. Chen, T.; Niu, R.-Q.; Li, P.-X.; Zhang, L.-P.; Du, B. Regional soil erosion risk mapping using RUSLE, GIS, and remote sensing: A case study in Miyun Watershed, North China. *Environ. Earth Sci.* **2011**, *63*, 533–541. [[CrossRef](#)]
3. Fang, G.; Yuan, T.; Zhang, Y.; Wen, X.; Lin, R. Integrated study on soil erosion using RUSLE and GIS in Yangtze River Basin of Jiangsu Province (China). *Arab. J. Geosci.* **2019**, *12*, 173. [[CrossRef](#)]
4. Fu, B.; Liu, Y.; Lü, Y.; He, C.; Zeng, Y.; Wu, B. Assessing the soil erosion control service of ecosystems change in the Loess Plateau of China. *Ecol. Complex.* **2011**, *8*, 284–293. [[CrossRef](#)]
5. Fu, B.J.; Zhao, W.W.; Chen, L.D.; Zhang, Q.J.; Lü, Y.H.; Gulinck, H.; Poesen, J. Assessment of soil erosion at large watershed scale using RUSLE and GIS: A case study in the Loess Plateau of China. *Land Degrad. Dev.* **2005**, *16*, 73–85. [[CrossRef](#)]
6. Sun, W.; Shao, Q.; Liu, J. Soil erosion and its response to the changes of precipitation and vegetation cover on the Loess Plateau. *J. Geogr. Sci.* **2013**, *23*, 1091–1106. [[CrossRef](#)]

7. Sun, W.; Shao, Q.; Liu, J.; Zhai, J. Assessing the effects of land use and topography on soil erosion on the Loess Plateau in China. *CATENA* **2014**, *121*, 151–163. [[CrossRef](#)]
8. Duan, X.; Xie, Y.; Ou, T.; Lu, H. Effects of soil erosion on long-term soil productivity in the black soil region of northeastern China. *CATENA* **2011**, *87*, 268–275. [[CrossRef](#)]
9. Yang, X.M.; Zhang, X.P.; Deng, W.; Fang, H.J. Black soil degradation by rainfall erosion in Jilin, China. *Land Degrad. Dev.* **2003**, *14*, 409–420. [[CrossRef](#)]
10. Lin, C.; Tu, S.; Huang, J.; Chen, Y. The effect of plant hedgerows on the spatial distribution of soil erosion and soil fertility on sloping farmland in the purple-soil area of China. *Soil Tillage Res.* **2009**, *105*, 307–312. [[CrossRef](#)]
11. Feng, T.; Chen, H.; Polyakov, V.O.; Wang, K.; Zhang, X.; Zhang, W. Soil erosion rates in two karst peak-cluster depression basins of northwest Guangxi, China: Comparison of the RUSLE model with <sup>137</sup>Cs measurements. *Geomorphology* **2016**, *253*, 217–224. [[CrossRef](#)]
12. Huang, W.; Ho, H.C.; Peng, Y.; Li, L. Qualitative risk assessment of soil erosion for karst landforms in Chahe town, Southwest China: A hazard index approach. *CATENA* **2016**, *144*, 184–193. [[CrossRef](#)]
13. Guo, B.; Zhou, Y.; Zhu, J.; Liu, W.; Wang, F.; Wang, L.; Jiang, L. An estimation method of soil freeze-thaw erosion in the Qinghai–Tibet Plateau. *Nat. Hazards* **2015**, *78*, 1843–1857. [[CrossRef](#)]
14. Wang, Y.; Wang, G.; Hu, H.; Cheng, H. Erosion rates evaluated by the <sup>137</sup>Cs technique in the high altitude area of the Qinghai–Tibet plateau of China. *Environ. Geol.* **2008**, *53*, 1743–1749. [[CrossRef](#)]
15. El Kateb, H.; Zhang, H.; Zhang, P.; Mosandl, R. Soil erosion and surface runoff on different vegetation covers and slope gradients: A field experiment in Southern Shaanxi Province, China. *CATENA* **2013**, *105*, 1–10. [[CrossRef](#)]
16. Li, J.; Ren, Z.; Zhou, Z. Ecosystem services and their values: A case study in the Qinba mountains of China. *Ecol. Res.* **2006**, *21*, 597–604. [[CrossRef](#)]
17. Xi, Z.D.; Sun, H.; Li, X.L. Characteristics of soil erosion and its Space-time Distributive pattern in Southern Mountains of Shaanxi Province. *Bull. Soil Water Conserv.* **1997**, *17*, 1–6.
18. Jia, T.M.; Du, S.T.; Zhou, L. Historical changes and eco-reestablishing strategy for Qinba mountain region. *J. Northwest Sci-Tech Univ. Agric. For. (Soc. Sci.)* **2002**, 12–16.
19. Wang, Z.J.; Su, Y.; Wang, Z.T. Characteristics of soil erosion in Wenchuanhe watershed of Hanjiang River based on GIS. *J. Northwest For. Univ.* **2016**, *31*, 199–205.
20. Wang, L.; Huang, J.; Yun, D.; Hu, Y.; Han, P. Dynamic Assessment of Soil Erosion Risk Using Landsat TM and HJ Satellite Data in Danjiangkou Reservoir Area, China. *Remote Sens.* **2013**, *5*, 3826–3848. [[CrossRef](#)]
21. Renard, K.G.; Foster, G.R.; Weesies, G.A.; McCool, D.K.; Yoder, D.C. Predicting soil erosion by water: A guide to conservation planning with the Revised Universal Soil Loss Equation (RUSLE). In *Agriculture Handbook*; U.S. Department of Agriculture (USDA): Washington, DC, USA, 1997.
22. Wischmeier, W.H.; Smith, D.D. Predicting rainfall erosion losses: A guide to conservation planning [USA]. In *Agriculture Handbook*; U.S. Department of Agriculture (USDA): Washington, DC, USA, 1978; p. 537.
23. Nearing, M.A.; Foster, G.R.; Lane, L.J.; Finkner, S.C. A Process-Based Soil Erosion Model for USDA-Water Erosion Prediction Project. *Trans. Am. Soc. Agric. Eng.* **1989**, *32*, 1587–1593. [[CrossRef](#)]
24. Kirkby, M.; Jones, R.J.A.; Irvine, B.; Gobin, A.G.G.; Cerdan, O.; Rompaey, V.J.J.; Bissonais, Y.L.; Daroussin, J.; King, D.; Montanarella, L. *Pan-European Soil Erosion Risk Assessment for Europe: The PESERA Map*, version 1 October 2003. Explanation of Special Publication Ispra 2004 No. 73 (S.P.I.04.73); European Communities: Luxembourg, 2004; Volume 39, pp. 36–40.
25. Cilek, A.; Berberoglu, S.; Kirkby, M.; Irvine, B.; Donmez, C.; Erdogan, M.A. Erosion Modelling In A Mediterranean Subcatchment Under Climate Change Scenarios Using Pan-European Soil Erosion Risk Assessment (PESERA). *Int. Arch. Photogramm. Remote Sens. Spat. Inf. Sci.* **2015**, *XL-7/W3*, 359–365. [[CrossRef](#)]
26. Karamesouti, M.; Petropoulos, G.P.; Papanikolaou, I.D.; Kairis, O.; Kosmas, K. Erosion rate predictions from PESERA and RUSLE at a Mediterranean site before and after a wildfire: Comparison & implications. *Geoderma* **2016**, *261*, 44–58.
27. Thomas, J.; Joseph, S.; Thrivikramji, K.P. Assessment of soil erosion in a tropical mountain river basin of the southern Western Ghats, India using RUSLE and GIS. *Geosci. Front.* **2018**, *9*, 893–906. [[CrossRef](#)]
28. Alkharabsheh, M.M.; Alexandridis, T.K.; Bilas, G.; Misopolinos, N.; Silleos, N. Impact of Land Cover Change on Soil Erosion Hazard in Northern Jordan Using Remote Sensing and GIS. *Procedia Environ. Sci.* **2013**, *19*, 912–921. [[CrossRef](#)]
29. Zhang, H.; Yang, Q.; Li, R.; Liu, Q.; Moore, D.; He, P.; Ritsema, C.J.; Geissen, V. Extension of a GIS procedure for calculating the RUSLE equation LS factor. *Comput. Geosci.* **2013**, *52*, 177–188. [[CrossRef](#)]

30. De Vente, J.; Poesen, J.; Verstraeten, G.; Govers, G.; Vanmaercke, M.; Van Rompaey, A.; Arabkhedri, M.; Boix-Fayos, C. Predicting soil erosion and sediment yield at regional scales: Where do we stand? *Earth-Sci. Rev.* **2013**, *127*, 16–29. [[CrossRef](#)]
31. Panagos, P.; Borrelli, P.; Poesen, J.; Ballabio, C.; Lugato, E.; Meusburger, K.; Montanarella, L.; Alewell, C. The new assessment of soil loss by water erosion in Europe. *Environ. Sci. Policy* **2015**, *54*, 438–447. [[CrossRef](#)]
32. Ganasri, B.P.; Ramesh, H. Assessment of soil erosion by RUSLE model using remote sensing and GIS—A case study of Nethravathi Basin. *Geosci. Front.* **2016**, *7*, 953–961. [[CrossRef](#)]
33. Borrelli, P.; Robinson, D.A.; Fleischer, L.R.; Lugato, E.; Ballabio, C.; Alewell, C.; Meusburger, K.; Modugno, S.; Schütt, B.; Ferro, V.; et al. An assessment of the global impact of 21st century land use change on soil erosion. *Nat. Commun.* **2017**, *8*, 2013. [[CrossRef](#)]
34. Fayas, C.M.; Abeysingha, N.S.; Nirmanee, K.G.S.; Samaratunga, D.; Mallawatantri, A. Soil loss estimation using rusle model to prioritize erosion control in KELANI river basin in Sri Lanka. *Int. Soil Water Conserv. Res.* **2019**, *7*, 130–137. [[CrossRef](#)]
35. Wijesundara, N.C.; Abeysingha, N.S.; Dissanayake, D.M.S.L.B. GIS-based soil loss estimation using RUSLE model: A case of Kirindi Oya river basin, Sri Lanka. *Modeling Earth Syst. Environ.* **2018**, *4*, 251–262. [[CrossRef](#)]
36. Pal, S.C.; Chakraborty, R. Simulating the impact of climate change on soil erosion in sub-tropical monsoon dominated watershed based on RUSLE, SCS runoff and MIROC5 climatic model. *Adv. Space Res.* **2019**, *64*, 352–377. [[CrossRef](#)]
37. Dabral, P.P.; Baithuri, N.; Pandey, A. Soil Erosion Assessment in a Hilly Catchment of North Eastern India Using USLE, GIS and Remote Sensing. *Water Resour. Manag.* **2008**, *22*, 1783–1798. [[CrossRef](#)]
38. Phinzi, K.; Ngetar, N.S. The assessment of water-borne erosion at catchment level using GIS-based RUSLE and remote sensing: A review. *Int. Soil Water Conserv. Res.* **2019**, *7*, 27–46. [[CrossRef](#)]
39. Zhang, W.B.; Xie, Y.; Liu, B.Y. Rainfall Erosivity Estimation Using Daily Rainfall Amounts. *Sci. Geogr. Sin.* **2002**, *6*, 53–56.
40. Williams, J.R.; Jones, C.A.; Dyke, P.T. A Modeling Approach to Determining the Relationship Between Erosion and Soil Productivity. *Trans. ASAE* **1984**, *27*, 129–144. [[CrossRef](#)]
41. Mccool, D.K.; Foster, G.R.; Mutchler, C.K.; Meyer, L.D. Revised Slope Length Factor for the Universal Soil Loss Equation. *Trans. ASAE* **1989**, *30*, 1387–1396. [[CrossRef](#)]
42. Liu, B.Y.; Nearing, M.A.; Shi, P.J.; Jia, Z.W. Slope Length Effects on Soil Loss for Steep Slopes. *Soil Sci. Soc. Am. J.* **2000**, *64*, 1759–1763. [[CrossRef](#)]
43. Zhou, Z.C.; Shangguan, Z.P.; Zhao, D. Modeling vegetation coverage and soil erosion in the Loess Plateau Area of China. *Ecol. Model.* **2006**, *198*, 263–268. [[CrossRef](#)]
44. Cai, C.F.; Ding, S.W.; Shi, Z.H.; Huang, L.; Zhang, G.Y. Study of Applying USLE and Geographical Information System IDRISI to Predict Soil Erosion in Small Watershed. *J. Soil Water Conserv.* **2000**, *14*, 19–24.
45. Duan, X.; Gu, Z.; Li, Y.; Xu, H. The spatiotemporal patterns of rainfall erosivity in Yunnan Province, southwest China: An analysis of empirical orthogonal functions. *Glob. Planet Chang.* **2016**, *144*, 82–93. [[CrossRef](#)]
46. Lai, C.; Chen, X.; Wang, Z.; Wu, X.; Zhao, S.; Wu, X.; Bai, W. Spatio-temporal variation in rainfall erosivity during 1960–2012 in the Pearl River Basin, China. *CATENA* **2016**, *137*, 382–391. [[CrossRef](#)]
47. Wang, Z.-J.; Jiao, J.-Y.; Rayburg, S.; Wang, Q.-L.; Su, Y. Soil erosion resistance of “Grain for Green” vegetation types under extreme rainfall conditions on the Loess Plateau, China. *CATENA* **2016**, *141*, 109–116. [[CrossRef](#)]
48. Dimotta, A.; Cozzi, M.; Romano, S.; Lazzari, M. *Soil Loss, Productivity and Cropland Values GIS-Based Analysis and Trends in the Basilicata Region (Southern Italy) from 1980 to 2013*, Cham, 2016; Springer International Publishing; Cham, Switzerland, 2016; pp. 29–45.
49. Dimotta, A.; Lazzari, M.; Cozzi, M.; Romano, S. *Soil Erosion Modelling on Arable Lands and Soil Types in Basilicata, Southern Italy*, Cham, 2017; Springer International Publishing; Cham, Switzerland, 2017; pp. 57–72.
50. Lazzari, M.; Gioia, D.; Piccarreta, M.; Danese, M.; Lanorte, A. Sediment yield and erosion rate estimation in the mountain catchments of the Camastra artificial reservoir (Southern Italy): A comparison between different empirical methods. *CATENA* **2015**, *127*, 323–339. [[CrossRef](#)]
51. Zhao, X.; Wu, P.; Gao, X.; Persaud, N. Soil Quality Indicators in Relation to Land Use and Topography in a Small Catchment on the Loess Plateau of China. *Land Degrad. Dev.* **2015**, *26*, 54–61. [[CrossRef](#)]
52. Römermann, C.; Dutoit, T.; Poschlod, P.; Buisson, E. Influence of former cultivation on the unique Mediterranean steppe of France and consequences for conservation management. *Biol. Conserv.* **2005**, *121*, 21–33. [[CrossRef](#)]

53. Zhao, W.Z.; Xiao, H.L.; Liu, Z.M.; Li, J. Soil degradation and restoration as affected by land use change in the semiarid Bashang area, northern China. *CATENA* **2005**, *59*, 173–186. [[CrossRef](#)]
54. Wang, Z.J.; Su, Y. Spatio temporal characteristics of land use change in southern Shaanxi Province in recent 20 years based on RS and GIS. *J. Nat. Disasters* **2017**, *26*, 164–174.
55. Wu, X.; Wang, X. Spatial Influence of Geographical Factors on Soil Erosion in Fuyang County, China. *Procedia Environ. Sci.* **2011**, *10*, 2128–2133. [[CrossRef](#)]



© 2020 by the authors. Licensee MDPI, Basel, Switzerland. This article is an open access article distributed under the terms and conditions of the Creative Commons Attribution (CC BY) license (<http://creativecommons.org/licenses/by/4.0/>).